Available online at www.sciencedirect.com
SCIENCE DIRECT®
NUCLEAR SCIENCE AND TECHNIQUES
Nuclear Science and Techniques, Vol.17, No.3 (2006) 164–169

High-resolution SPECT for small-animal imaging

QI Yu-Jin
(Shanghai Institute of Applied Physics, the Chinese Academy of Sciences, Shanghai 201800, China)

Abstract This article presents a brief overview of the development of high-resolution SPECT for small-animal imaging. A pinhole collimator has been used for high-resolution animal SPECT to provide better spatial resolution and detection efficiency in comparison with a parallel-hole collimator. The theory of imaging characteristics of the pinhole collimator is presented and the designs of the pinhole aperture are discussed. The detector technologies used for the development of small-animal SPECT and the recent advances are presented. The evolving trend of small-animal SPECT is toward a multi-pinhole and a multi-detector system to obtain a high resolution and also a high detection efficiency.

Key words Small-animal SPECT, Molecular imaging, Pinhole collimation, Gamma camera
CLC numbers R817.4, TB811$^+$.2

1 Introduction

The rapid advance in molecular biology and the increasing use of transgenic mice as models of human biology and diseases have led to significant interests in the development of noninvasive, high-resolution, *in vivo* imaging techniques for small animals[1-4]. Medical imaging techniques including ultrasound (US), computed tomography (CT), magnetic resonance imaging (MRI), positron emission tomography (PET), and single-photon emission computed tomography (SPECT), are contributing to this new field[1,4], each with its unique mechanisms for generating contrast and trade-offs in spatial resolution and sensitivity with respect to the biological process of interest[1].

In humans, SPECT has been used for a variety of routine clinical applications including myocardial perfusion, bone metabolism, brain function, tumor imaging, etc. The principal advantages of SPECT over other imaging modalities are that the imaging systems are less expensive and the imaging agents have a longer life and thus are easier and cheaper to distribute. The advantage of SPECT over PET is the fact that there is no inherent limit on the obtainable spatial resolution. However, the use of gamma collimators results in considerably reduced efficiency for SPECT when compared with PET.

Clinical SPECT using a conventional gamma camera fitted with a parallel-hole collimator is severely limited by the trade-off between spatial resolution and detection efficiency. The intrinsic spatial resolution of gamma cameras ($\sim$4 mm for modern cameras) imposes additional limitations on the achievable image resolution. To image small animals such as mice, very high resolution (less than 1 mm) is often required, which is very difficult to achieve for the conventional SPECT. However, the use of pinhole collimators to image small objects allows high-resolution images with feasible acquisition time and injected activities. Therefore, the pinhole collimator has been proposed to develop high-resolution SPECT systems for small-animal imaging[5-7].

There are two main implementation approaches to develop high-resolution pinhole SPECT systems. One is to use a conventional gamma camera with a continuous scintillation crystal [8-10], which has a large

Partially supported by National Science Foundation of China (Grant No. 30570520).
Received date: 2006-03-06

field-of-view (~ 40 cm) but poor intrinsic spatial resolution (~ 4 mm). The other is to develop a compact modular gamma camera with a pixellated crystal array, which has a better intrinsic spatial resolution ($\sim 1-2$ mm) but a relatively small field-of-view (~ 10 cm)[11-14]. The standard camera needs a larger pinhole collimator to provide a higher magnification to overcome the limitation of the poor intrinsic spatial resolution. On the contrary, a modular camera allows the use of a smaller pinhole collimator with lower magnification. Its compact size and light weight have a great advantage in the configuration of a multiple-head pinhole SPECT system.

In this article, we present a brief overview of the developments of high-resolution SPECT for small-animal imaging. The theory of imaging characteristics of a pinhole collimator is introduced first, and then the designs of the pinhole collimator are discussed. The instrumentations of a high-resolution compact gamma camera are introduced. Finally, the recent advance of small-animal SPECT is presented.

2 Pinhole imaging characteristics and collimator designs

The imaging geometry of the pinhole collimator as compared to that of the parallel-hole collimator is shown in Fig.1. The object is positioned close to the pinhole aperture, and a reversed and magnified image is projected onto the detector. Comprehensive discussions of the principle of pinhole imaging in nuclear medicine can be found in Anger[15] and Barrett and Swindell[16]. The unique feature of pinhole imaging is that the image is magnified as compared to the image of the parallel-hole collimator. Due to this magnification, the limits imposed by the intrinsic resolution of the camera system would be overcome. In addition, the pinhole collimator also provides a better trade-off between image resolution and photon detection efficiency than the parallel-hole collimator.

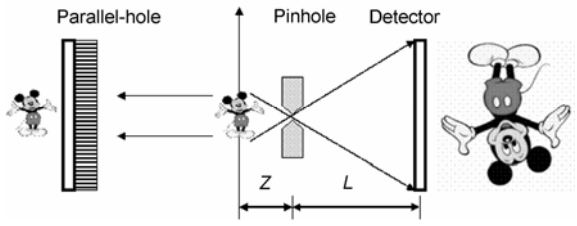

Fig. 1 Schematic view of pinhole imaging as compared with parallel-hole collimator.

2.1 Imaging characteristics of the pinhole collimator

From the basic pinhole geometry shown in Fig. 1, the geometric efficiency G of the pinhole collimator for an object placed at a distance z from the collimator is given by[17]

$$G = \frac{a_e^2 \cos^3 \theta}{16 z^2} \tag{1}$$

where z is the object-to-collimator distance, θ is the angle between the axis of the collimator and the line joining the center of the pinhole to the point source, and a_e is the effective diameter of the pinhole aperture, which is given by

$$a_e = \sqrt{a\left(a + \frac{2\tan(\Omega/2)}{\mu}\right)} \tag{2}$$

where a is the diameter of the pinhole aperture, Ω is the cone angle of the pinhole collimator, and μ is the linear attenuation coefficient of the aperture material at the photon energy. Eq. (1) shows that the geometric efficiency decreases rapidly as a function of the distance between the source and the pinhole aperture (i.e., proportional to $1/z^2$), and the oblique angle of incidence of the photon.

The geometric spatial resolution of a pinhole aperture in the axial direction (perpendicular to the detector face) is given by

$$R_o = \frac{a_e (L+z)}{L} \tag{3}$$

where z is the object-to-collimator distance, L is the collimator length, and a_e is the effective hole diameter of the pinhole aperture.

The total spatial resolution at the object plane taking into account the intrinsic resolution of the camera is given by

$$R_T = \sqrt{R_o^2 + \left(\frac{z}{L}\right)^2 R_i^2} = \sqrt{R_o^2 + \left(\frac{R_i}{M}\right)^2} \tag{4}$$

where R_o is given by Eq. (3), R_i is the intrinsic resolution of the detector, and $M = L/z$ is the image magnification factor. According to Eq. (4), by choosing sufficient magnification to overcome the limit of the detector intrinsic resolution, the resolution of pinhole imaging is only limited by the size of the pinhole aperture, the gamma photon energy, and the material

used to fabricate the pinhole aperture.

Fig.2 shows the plot of the resolution of a pinhole collimator as a function of object magnification *M*, with different pinhole aperture sizes for a detector with 1.5 mm pixel pitch. The figure shows improvement in resolution as the magnification increases for any given aperture size. At high magnification, the resolution improvement levels off as the pinhole size becomes a dominating factor in determining the resolution of the pinhole collimator.

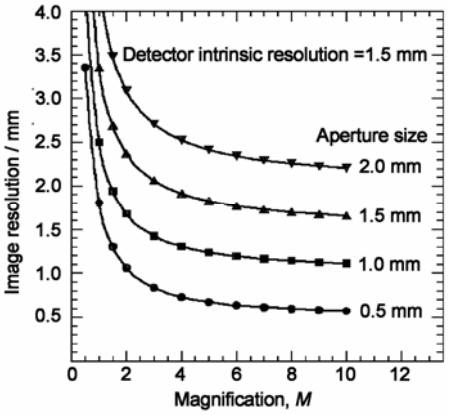

Fig. 2 Image resolution versus magnification for various pinhole sizes over a broad magnification range for small-animal imaging.

2.2 Designs of the pinhole aperture

The above formulations provide theoretical predictions of the performance characteristics of a pinhole collimator with a specific aperture size. These are useful in designing the pinhole aperture. However, these equations assume that the material used in the aperture is perfectly opaque to the radiation used. In practice, especially in high-resolution pinhole imaging using higher energy photons, penetration through and scatter by the pinhole aperture have significant effects on the performance of this imaging technique. Recently, analytic formulations for the pinhole resolution including penetration have been developed[18, 19]. For an optimized collimator design, Monte Carlo (MC) simulation methods are often used because they allow a more detailed and precise assessment of the imaging characteristics of pinhole collimators [20, 21]. In particular, they provide information about the geometric component, the penetration and scatter components of the response function of the pinhole collimator.

In practice, the design of the pinhole aperture is required to be optimized according to gamma energy. There are two types of pinhole aperture designs, shown in Fig.3. One is the knife-edge design for low-energy gamma rays, and the other is the keel-edge design[22] for medium and high energy gamma rays. Due to the height of the channel in the keel-edge design, gamma-ray penetration through the pinhole aperture can be greatly reduced.

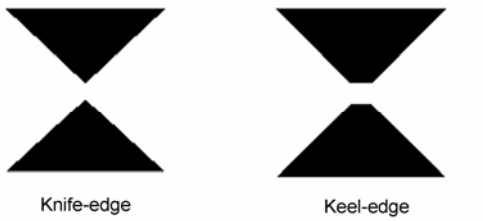

Fig.3 Two types of pinhole aperture designs with knife-edge (left) and keel-edge (right).

3 Dedicated small-animal detectors

Even though clinical gamma cameras are applicable to small-animal SPECT by using pinhole collimators, there is still considerable motivation for developing dedicated gamma-ray detectors for this application. The goals of this endeavor are to produce inexpensive, high-resolution modules that are well suited to small animals.

Two kinds of detector technologies are commonly used in the development of modular gamma cameras for high-resolution small-animal SPECT. One is based on the pixellated scintillators coupled to photo-detectors such as position-sensitive photomultiplier tubes (PSPMTs), arrays of compact PMTs, or PIN photodiode arrays[23-26]. The other is based on solid-state detectors such as arrays of cadmium telluride (CdTe) or cadmium-zinc-telluride (CZT)[27, 28]. Several research groups have built dedicated small-animal SPECT systems using this technology for small animal imaging[13, 14, 29]. Fig. 4 shows a desktop small-animal SPECT system developed in the research group led by Dr. Benjamin Tsui at Johns Hopkins University[14]. This system was designed such that the camera-head was placed in a stationary position and the imaging object was rotated vertically in front of the collimator. The image resolution was achieved between 1mm and 1.5mm[14]. Commercial small-animal SPECT systems, A-SPECT® and X-SPECT®, from Gamma Medica Inc. also use the same technology [12, 30].

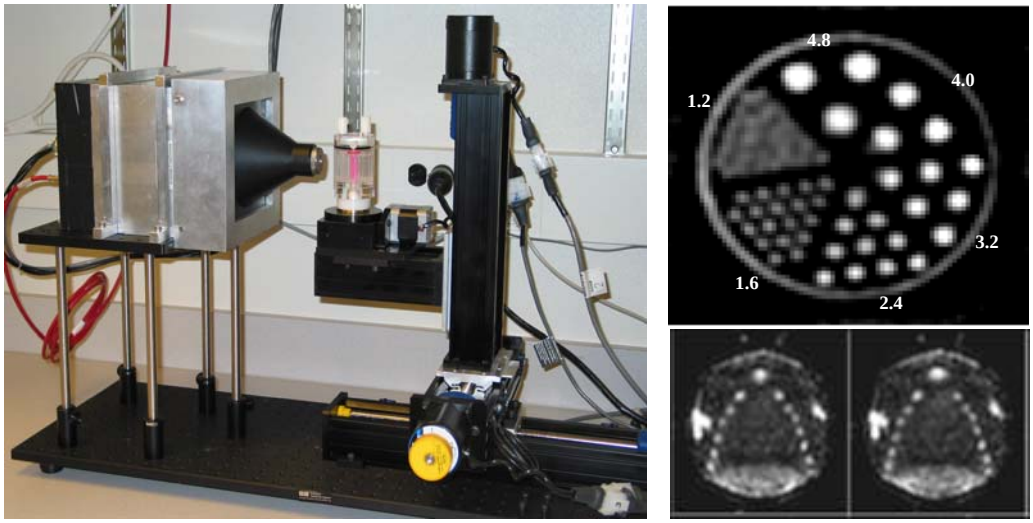

Fig. 4 A photograph of the JHU's small-animal SPECT system based on a modular gamma camera using pixellated Na(Tl) crystal array and 5" Hamamatsu R3292 PSPMT. The right top is the transaxial image of a Jaszczak phantom with 5 cm diameter and the right bottom is the coronal image slice through the chest of a 30-g mouse injected with ^{99m}Tc-MDP[14].

The latest PSPMT technology, such as the compact H9500 flat panel PSPMT from Hamamatsu, and the availability of pixellated scintillation arrays with smaller (< 1 mm) pixels provide a unique opportunity to implement a new generation of high-performance compact gamma cameras for high-resolution pinhole SPECT imaging.

Recently, the research group led by Dr. Harrison Barrett at the University of Arizona constructed a compact small-animal SPECT/CT system[28], shown in Fig. 5, using a 2" modular CZT detector. This CZT detector consists of a $25\,\text{mm} \times 25\,\text{mm} \times \sim 2\,\text{mm}$ CZT crystal, which was patterned with a 64×64 array of pixel electrodes with a pixel pitch of 0.38 mm. Although the system offers very high intrinsic spatial resolution, the detector's field-of-view (FOV) is insufficient for small-animal imaging. Since CZT detectors with larger FOV are still difficult and expensive to produce, a modular camera system based on semiconductor detectors is still a costly alternative to a system based on pixellated scintillators.

Despite their better energy resolution and potentially higher spatial resolution as compared with scintillation detectors, solid-state detector technologies, such as CZT, continue to struggle with several challenges. These include difficulty in producing a reliably large-area crystal, low yields in growing high-quality crystals, and issues of pixel response uniformity and operational stability with time.

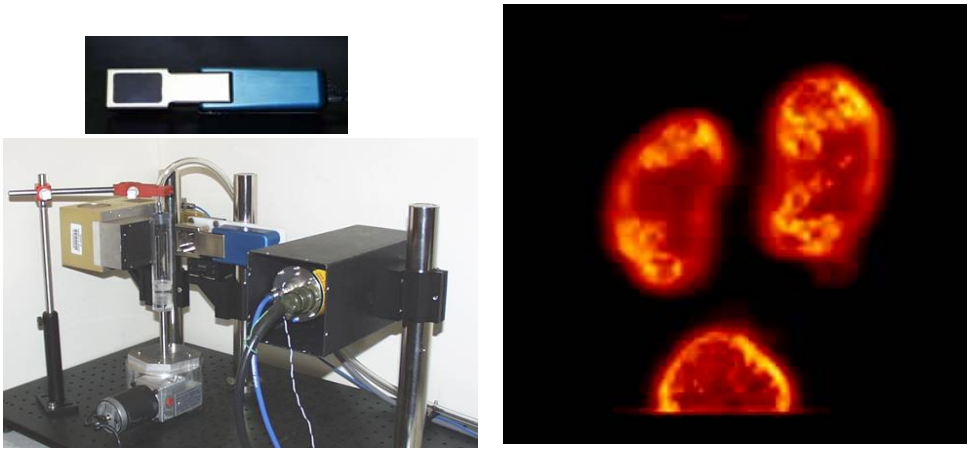

Fig. 5 A compact small-animal SPECT/CT system combines a CZT SpotImager (left top) with a transmission X-ray system. The imaging subject is rotated vertically. The right panel shows a mouse kidney image volume rendering from SPECT imaging with ^{99m}Tc-glucarate. (The pictures are taken from the website of the Center of Gamma-Ray Imaging at Arizona University).

4 Recent advances in small-animal SPECT

In small-animal SPECT, discussed in the previous section, the limitations currently are related largely to the sensitivity. As for the traditional approach in pinhole-aperture designs with a fixed imaging geometry, there is an inevitable trade-off between the photon collection efficiency and the spatial resolution: a smaller pinhole improves resolution but degrades efficiency. A number of novel collimation techniques are being explored that can simultaneously provide a high resolution and a high collection efficiency of the gamma photons by using multiple pinhole collimation[31, 32] or code aperture methods[33, 34].

Recent advances in small-animal SPECT instrumentation is the implementation of multiple pinhole collimators with multidetectors to provide both high spatial resolution (sub-millimeter) and high sensitivity for small-animal SPECT imaging. Several such systems are under construction. The SemiSPECT system, comprising eight CZT hybrid detectors in compact housing, is under development in the Center of Gamma-Ray Imaging (CGR), of Arizona University at Tucson, USA. Each modular detector consists of a 26.9 mm × 26.9 mm × ~2 mm CZT crystal, which was patterned with a 64 × 64 array of pixel electrodes with a pixel pitch of 0.38 mm. This system is dedicated for mice imaging. Another system is the U-SPECT (Fig.6) [35], which is under construction at the Medical Center of Utrench University, Netherland. It has nine rings with 20 micropinholes each to acquire nonoverlap projection data and it aims to achieve 0.1 microliter image resolution[36].

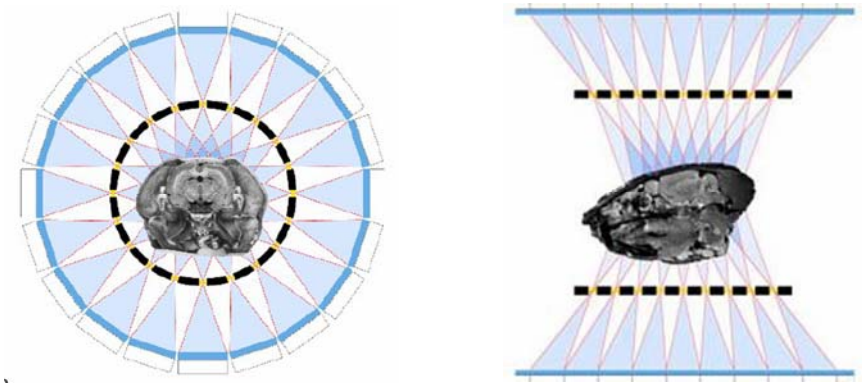

Fig. 6 A schematic view of U-SPECT developed at the Utrench University, Netherland. It has nine rings and each ring has 20 micropinholes to acquire nonoverlap projection data[35].

In summary, small-animal SPECT is advancing rapidly. Besides the innovations in image formation collimators, more advanced detection technologies developed in nuclear physics and high-energy physics are being applied to this field so that the resolution of the image system falls within the limit of the detectors. The evolving trend in small-animal SPECT is multipinhole and multidetector systems.

Acknowledgments

The author acknowledges the immense wealth of information gained from valued colleagues in academia, industry, and the clinical nuclear medicine community from all over the world. The help of Dr. Benjamin Tsui, Johns Hopkins University; Dr. Stan Majewski, Jefferson National Lab; and Dr. Randy Wojick, Ray Vision Inc. is acknowledged.

References

1 Cherry S R, Phys. Med. Biol. 2004, **49**:R13-R48.

2 Weissleder R, Mahmood U, Radiology, 2001, **219:**316-333.

3 Weissleder R, Cancer Reviews, Nature, 2002, **2:**1-8.

4 Budinger T F, Benaron D A, Koretsky A P, Annual Review, Annu. Rev. Biomed. Eng. 1999, **1:** 611-648.

5 Weber D A, Ivanovic M, Franceschi D, *et al.* Journal of Nuclear Medicine, 1994, **35:** 342-348.

6 Jaszczak R, Li J, Wang H, *et al.* Phys Med Biol, 1994, **39:** 425-443.

7 Weber D A, Ivanovic M, Journal of Nuclear Medicine, 1995, **36:** 2287-2289.

8 Yokoi T, Kishi H, Kaku Igaku - Japanese Journal of Nuclear Medicine, 1998, **35:** 901-907.

9 Wu M C, Tang H R, O'Connell J W, *et al.* IEEE Transactions on Nuclear Science, 1999, **46:** 1199-1202.

10 Tsui B M W, Wang Y, Frey E C, *et al*. Journal of Nuclear Medicine, 2001, **42**(5): 54P-55P.

11 Kastis G A, Barber H B, Barrett H H, *et al*. Journal of Nuclear Medicine, 1998, **39:** 9P.

12 McElroy D P, MacDonald L R, Beekman F J, *et al*. IEEE Trans. Nucl. Sci., 2002, **49:** 2139-2147.

13 Wojcik R, Goode A R, Smith M, *et al*. IEEE Nuclear Science Symposium Conference Record, 2003, **3:** 1819-1823.

14 Qi Y J, Tsui B M W, Wang Y, *et al.* Development and characterization of a high-resolution microSPECT system for small animal imaging, In: Kupinski M A, Barrett H H (ed), Small-animal SPECT imaging, Springer Press, 2005: 259-266,.

15 Anger H O, Radioisotope cameras, In: Instrumentation in nuclear medicine, Vol.1, Hine G J, ed. New York: Academic Press, 1967: 485-552.

16 Barrett H H, Swindell W, Radioological imaging: The theory of imaging formation, detection, and processing, Vol. 1 & 2, New York: Academic Press, 1981.

17 Tsui B M W, Gunter D, Beck R, *et al*. Physics of collimator design, In: Sandler C R, Wackers FJTh, Patton J A, *et al*. (ed). Diagnostic nuclear medicine, Vol. 1, Third Edition, Baltimore William and Wilkins, 1996: 67- 80.

18 Metzler S D, Bowsher J E, Smith M F, *et al.* IEEE Transactions on Medical Imaging, 2001, **20**(8): 730-741.

19 Metzler S D, Bowsher J E, Greer K L, *et al*. IEEE Transactions on Medical Imaging, 2002, **21:** 878-887.

20 Gieles M, de Jong H W A M, Beekman F J. Phys. Med. Biol. 2002, **47**(11): 1853-1867.

21 Qi Y, Tsui B M W, Wang Y, *et al*. Journal of Nuclear Medicine, 2004, **45** (5), Suppl: 442.

22 Smith M F, Jaszczak R J, Wang H.,. IEEE Transactions on Nuclear Science, 1997, **44**(3): 1154-1160.

23 Wojcik R, Majewski S, Steinbach D, *et al*. IEEE Transactions on Nuclear Science, 1998, **45**(3): 487-491.

24 Weisenberger A G, Kross B, Majewski S, *et al*. IEEE Transactions on Nuclear Science, 1998, **45**(6): 3053-3058.

25 Pani R, Soluri A, Scafe R, *et al*. IEEE Transactions on Nuclear Science, 1999, **46:** 702-708.

26 Levin C S, Hoffman E J, Tornai M P, *et al*. IEEE Transactions on Nuclear Science, 1997, **44**(4): 1513-1520.

27 Kastis G A, Barber H B, Barrett H H, *et al.* IEEE Transactions on Nuclear Science, 2000, **47:** 1923-1927.

28 Kastis G A, Furenlid L R, Wilson D W, *et al.* IEEE Transactions on Nuclear Science, 2004, **51:** 63-67.

29 Weisenberger A G., Wojcik R., Bradley E L, *et al.* IEEE Transactions on Nuclear Science, 2003, **50:** 74-79.

30 MacDonald L R, Patt B E, Iwanczyk J S, *et al*. IEEE Transactions on Nuclear Science, 2001, **48:** 830-836.

31 Schramm N U, Ebel G, Engeland U, *et al.* IEEE Transactions on Nuclear Science, 2003, **50:** 315-320.

32 Mok Seng Peng, Tsui M W, Wang Yuchuan, *et al.* IEEE Nuclear Science Symposium Conference Record, 2004, **6:** 3340-3444.

33 Meikle S R, Kench P, Weisenberger A G, *et al*. IEEE Transactions on Nuclear Science, 2002, **49:** 2167-2171.

34 Accorsi R, Gasparini F, Lanza R C. IEEE Transactions on Nuclear Science, 2001, **48**(6): 2411-2417.

35 Beekman F J, Vastenhouw B, IEEE Nuclear Science Symposium Conference Record, 2002, **2**: 792-796.

36 Beekman F J, van der Have F, Vastenhouw B, *et al*. Journal of Nuclear Medicine, 2005, **46:** 1194-1200.